Environ Sci Pollut Res (2017) 24:17790–17804
DOI 10.1007/s11356-017-9419-1

RESEARCH ARTICLE

Removal of cationic pollutants from water by xanthated corn cob: optimization, kinetics, thermodynamics, and prediction of purification process

Miloš Kostić[1] · Miloš Đorđević[1] · Jelena Mitrović[1] · Nena Velinov[1] · Danijela Bojić[1] · Milan Antonijević[2] · Aleksandar Bojić[1]

Received: 10 January 2017 / Accepted: 30 May 2017 / Published online: 11 June 2017

Abstract The removal of Cr(III) ions and methylene blue (MB) from aqueous solutions by xanthated corn cob (xCC) in batch conditions was investigated. The sorption capacity of xCC strongly depended of the pH, and increase when the pH rises. The kinetics was well fitted by pseudo-second-order and Chrastil's model. Sorption of Cr(III) ions and MB on xCC was rapid during the first 20 min of contact time and, thereafter, the biosorption rate decrease gradually until reaching equilibrium. The maximum sorption capacity of 17.13 and 83.89 mg g^{-1} for Cr(III) ions and MB, respectively, was obtained at 40 °C, pH 5, and sorbent dose 4 g dm^{-3} for removal of Cr(III) ions and 1 g dm^{-3} for removal of MB. The prediction of purification process was successfully carried out, and the verification of theoretically calculated amounts of sorbent was confirmed by using packed-bed column laboratory system with recirculation of the aqueous phase. The wastewater from chrome plating industry was successfully purified, i.e., after 40 min concentration of Cr(III) ions was decreased lower than 0.1 mg dm^{-3}. Also, removal of MB from the river water was successfully carried out and after 40 min, removal efficiency was about 94%.

Responsible editor: Guilherme L. Dotto

Electronic supplementary material The online version of this article (doi:10.1007/s11356-017-9419-1) contains supplementary material, which is available to authorized users.

✉ Miloš Kostić
mk484475@gmail.com

[1] Department of Chemistry, Faculty of Science and Mathematics, University of Niš, Višegradska 33, 18000 Nis, Serbia

[2] Faculty of Engineering and Science, University of Greenwich, Chatham Maritime, Kent, ME4 4TB, UK

Keywords Xanthated biomaterial · Cr(III) · Methylene blue · Sorption · Thermodynamics · Wastewater

Introduction

Heavy metals are toxic pollutants and non-biodegradable, which can accumulate in living tissues causing various diseases and disorders. Apart the esthetic problems, the greatest environmental concern with dyes is their inhibitory effect on photosynthesis in aquatic ecosystems. The effective removal of heavy metals and dyes from aqueous waste is among the most important issues of the world. Electroplating, leather tanning and dyeing, mining or pigment, wood preservation, battery manufacturing, and textile industries are examples of industries that release a high volume of wastewater containing heavy metals and dyes into the environment and aquatic ecosystems. Trivalent chromium, Cr(III), is required for metabolism sugar and fat metabolism in organisms (Anderson 1997), but long-time exposure causes skin allergic and cancer (Gupta et al. 2011; Rajurkar et al. 2011; Yun et al. 2001). Methylene blue (MB) is a thiazine (cationic) dye; it is not regarded as acutely toxic, but it has various harmful effects (eye burns, may cause nausea, vomiting, and gastritis problems) (Haque et al. 2002).

The most common method for heavy metal removal from wastewater is chemical precipitation. Low chromium content in water leads to an increase of precipitant in the process of chromium removal. Furthermore, the precipitation process generates the toxic sludge that has to be dewatered, stabilized, and disposed of. Chromium will only precipitate in the trivalent form, and thus, it must be reduced from its hexavalent form prior to precipitation. Hexavalent chromium reduction is achieved at low pH levels (~2–3) with a reducing agent-usually sodium metabisulfite or ferrous sulfite (Naja and Volesky 2009).

If the pH is maintained between 8.2 and 8.6, then the trivalent chrome will be precipitated as the hydroxide. This method produces an effluent containing trivalent chromium between 2 and 5 mg dm^{-3} (Bennett 2001). Trivalent chromium cannot be removed by precipitation below the maximum permissible limits. The US Environmental Protection Agency (EPA) and The World Health Organization (WHO) recommended the maximum permissible limits of chromium (as total chromium) in drinking water of 0.1 and 0.05 mg dm^{-3}, respectively (Rajput and Pittman 2015). Among the various water treatment techniques, sorption is generally preferred for the removal of heavy metal ions and other hazardous materials, especially at the concentrations ranging from 1 to 100 mg dm^{-3}, because of its high efficiency, minimization of chemicals, easy handling, availability of different sorbents, cost-effectiveness, and higher effectiveness than the conventional methods such as chemical precipitation and ion exchange (Schiewer and Volesky 1995). Sorption is a physicochemical process by which one substance becomes attached to another (Michalak et al. 2013). Biosorbent or biological matrix has been proposed as one of the most promising technologies for the removal of heavy metal and dyes ions from wastewaters (Wang and Chen 2009). In recent years, a number of agricultural and forestry by-products such as Soybean meal (Witek-Krowiak and Harikishore Kumar Reddy 2013), saltbush (*Atriplex canescens*) (Sawalha et al. 2006), blue-green algae *Spirulina* sp. (Chojnacka et al. 2005), rose petals biomass (Iftikhar et al. 2009), and bacterial dead *Streptomyces rimosus* biomass (Selatnia and Bakhti 2005) have been used for the removal of Cr(III) ions from water solution. Methylene blue is selected as a model compound in order to evaluate the capacity of biosorbent. Many textile manufacturers use and release aromatic amines (e.g., benzidine, methylene), and they are potential carcinogens (Raval et al. 2016), wherefore the attention is focused on the removal of dye from aqueous solutions. The biosorption mechanisms depend on the type of functional groups on the surface of the biomass and the nature of the metal. The main goal of such studies is to examine the possibilities for producing novel and cheaper forms of sorbents with standard or even better properties. The majority of biosorbents explored in previous studies were small particles with low density, poor mechanical strength, and small hardness, which resulted in difficult post-separation of the treated effluent from the biosorbents especially in the practical application.

The aim of this work is synthesis of new xanthated biosorbent based on corn cob. In this biosorbent, xanthate groups (strong acid) are introduced in the structure of basic corn cob biomass by xanthation and sorption characteristics and abilities of material were improved. These negatively charged groups have a high affinity for binding of cations. Obtained biosorbent will be applied for the removal of Cr(III) ions and methylene blue (MB) from aqueous solutions. There are no studies of the Cr(III) ions and methylene blue removal by xanthated biosorbents, especially corn cob, as well as use of xanthated biosorbents for wastewater purification. Xanthated corn cob (xCC) shows higher affinity and sorption capacity (about five times higher) for binding Cr(III) ions and methylene blue than basic corn cob biosorbent (CC), which predominantly has only weak acid carboxylic and phenolic groups.

The effect of various experimental parameters on the biosorption removal of Cr(III) and MB by xCC, such as contact time, initial pH, initial metal ion concentration, biosorbent dose, particle size, temperature, and stirring speed, were investigated. Biosorption process was described by fitting the experimental points using equilibrium, kinetic, and thermodynamic models. Obtained kinetic and equilibrium experimental data were modeled by non-linear fitting which better represents real conditions and phenomena which happen during sorption process than in linear models (Ho 2006). In order to determine the rate-controlling step in the overall process of biosorption, kinetic data were also examined by intraparticle diffusion model and Chrastil's model. Scanning electron microscopy (SEM), energy dispersive X-ray analysis (EDX), and Fourier transform infrared spectroscopy (FTIR) were used to investigate characteristics of xanthated biosorbent (xCC) and its interaction with Cr(III) ions and MB. In this work will be also presented new specific laboratory system for biosorption treatment. This laboratory system can be directly used for continuous process of purification in rinsing water baths in galvanization and similar processes. This work includes prediction and designing of purification process based on detailed equilibrium studies and mathematical tools for results interpretation.

Materials and methods

Reagents

All chemicals were of reagent grade and used without further refinement. HNO_3, NaOH, CS_2, and $Cr(NO_3)_3{\cdot}9H_2O$ were purchased from Merck (Germany). All solutions were prepared with deionized water (18 MΩ). Methylene blue (Riedel de Haen, Germany) was used without further purification. Standard metal and dye stock solution was prepared by dissolving given amounts of pure $Cr(NO_3)_3{\cdot}9H_2O$ and methylene blue. All standard solutions were stored in a refrigerator at +4 °C.

Preparation of xanthated biosorbent

Corn cob (*Zea mays*) used in the preparation of the xanthated biomass was harvested in October from a field near the town of Niš in Serbia. *Z. mays* was roughly crushed, washed with

deionized water, and grounded by laboratory mill (Waring, Germany). *Z. mays* were initially treated with diluted nitric acid and after that by sodium hydroxide, producing a basic CC (Stanković et al. 2012). Dried corn cob biomass was fractionized using standard sieves (Endecotts, England). Xanthation was carried out by following procedure: 10 g basic biomass, with granulation from 0.8 to 1.25 mm, was soaked in 5 mol dm^{-3} NaOH, stirred for 90 min, and washed with deionized water. This material was then esterified with 1.0 cm^3 of CS_2 and 50 cm^3 2.5 mol dm^{-3} NaOH for another 180 min. Xanthated material was allowed to settle and separated by decantation and filtration. Synthesized xanthate was washed with water several times to remove excess alkali until pH of water became neutral, which was followed by washing with acetone. The material was stored in an airtight plastic container for further use (Kostić et al. 2013).

Batch biosorption experiments

Batch mode sorption experiments were carried out with 1.0 g sorbent in 250 cm^3 of Cr(III) solution and 0.25 g sorbent in 250 cm^3 of MB solution and 250 cm^3 of in 400-cm^3 Erlenmeyer flasks with an agitation rate of 200 rpm and temperature 20 °C. To study the effect of pH, the Cr(III) and MB solution (50 and 100 mg dm^{-3}, respectively) was adjusted to the desired pH (2.0–6.0 for Cr(III) ions and 2–10 for MB) with HNO_3 or NaOH using a pH-meter (SensIon5, HACH, USA). The pH was maintained during treatment and kept to within ±0.2 U by adding 0.01 or 0.1 mol dm^{-3} HNO_3 in small portions. The effect of particle size xCC on biosorption was assessed in Cr(III) and MB solution at 50 mg dm^{-3} initial Cr(III) concentration and 100 mg dm^{-3} MB, pH 5.0, with different particle sizes ranging from 0.1–0.4 mm to 2.5–4.0 mm, at 20 °C and stirring speed 200 rpm. The effect of variation in the sorbent dose from 0.5 to 8 g dm^{-3} on the sorption of 50 mg dm^{-3} initial Cr(III) concentration and 100 mg dm^{-3} MB at constant values of pH 5 and stirring speed 200 rpm was studied. The effect of stirring speed (the stirring speed varied from 50 to 600 rpm) on removal of Cr(III) ions and MB with xCC biomass was carried out at pH 5.0 using 50.0 mg dm^{-3} Cr(III) and 100 mg dm^{-3} MB solutions. For the equilibrium and kinetic biosorption studies, xCC biomass (4 g dm^{-3}) was mixed with Cr(III) solution of different initial Cr(III) concentrations (10, 20, 50, 100, 200, and 400 mg dm^{-3}) and xCC biomass (1 g dm^{-3}) was mixed with MB solution of different initial MB concentrations (100, 150, 200, 250, and 400 mg dm^{-3}) at 10, 20, 30, and 40 °C in thermostated bath (Refrigerated/Heating Circulator, Julabo F12-ED, Germany), with constant agitation at 200 rpm for 180 min to ensure biosorption equilibrium. Residual Cr(III) ions concentrations in all samples were measured using air–acetylene flame atomic absorption spectrometer. Residual MB concentrations in all samples were measured using UV–Vis spectrophotometer. The amount of metal and dye sorbed q_t (mg g^{-1}) was determined by using the following equation

$$q_t = \frac{(c_0 - c_t) \times V}{m} \quad (1)$$

where c_0 and c_t are the initial and final concentrations of the metal ion and dye in solution (mg dm^{-3}), V is the solution volume (dm^3), and m is the mass of the sorbent (g).

The removal efficiency (RE) of metal ions and dye was calculated using Eq. 2

$$\mathrm{RE}\% = \frac{c_0 - c_t}{c_0} \times 100 \quad (2)$$

where c_0 and c_t are the initial and final concentrations of the metal ion and dye in the solution (mg dm^{-3}), respectively.

The prediction of purification process and verification of theoretically calculated amounts of sorbent for purification of wastewater were carried out in batch conditions, i.e., laboratory system with packed-bed column and recirculation of the aqueous phase. The sorption experiments were conducted in a transparent cylindrical polypropylene column. Appropriate, i.e., calculated amount of xCC was packed between two discs of sintered alumina into a 200-mm-length column. Cr(III) ions and MB solutions were pumped from the bottom of the column to the top using a peristaltic pump model SP 311 (VELP Scientifica, Italy). Samples were collected from the exit of the column after 0, 1, 5, 10, 20, 40, 90, 120, and 180 min and analyzed for the residual concentrations of Cr(III) ions and MB, as described above. The different volumes of the wastewater (from 1 to 5 dm^3) and desired removal efficiency were simulated in order to predict the required amount of sorbent for subsequent purification of wastewater with known concentration of Cr(III) ions and MB (114 mg dm^{-3} for Cr(III) ions and 100 mg dm^{-3} for MB).

Analysis

Cr(III) concentrations in the samples were measured using atomic absorption spectrophotometry (AAnalyst 300; PerkinElmer, USA), after filtration through a 0.45-μm membrane (Agilent Technologies, Germany). MB concentrations of the samples were measured using spectrophotometer Shimadzu UV–Vis 1650 PC (Shimadzu, Japan). Infrared spectrum of native biomass and xCC was obtained using a Fourier transform infrared spectrometer (Bomem Hartmann & Braun MB-100 spectrometer). The morphology of the xCC surface was analyzed by scanning electron microscopy (SEM) (Hitachi SU8030). EDX analysis (Thermo Scientific NORAN System 7, USA) provides elemental information via analysis of X-ray emissions from the sorbent surface.

Elemental composition was analyzed by elemental analysis on a PerkinElmer series II CHNS/O System Analyzer 2400.

Results and discussion

FTIR, SEM, and EDX characterizations of the xCC

FTIR analysis of basic CC and xCC is represented in Fig. 1. The very strong sorption band at around 3438 cm^{-1} from CC corresponds to hydroxyl groups on the biomass surface. The sorption band around 2921 cm^{-1} for basic CC corresponds to C–H stretching of CH_2 groups. The peaks near 1636 and 1458 cm^{-1} for CC are due to asymmetric and symmetric stretching vibration of C=O in ionic carboxylic groups (–COO–). Aliphatic acid group vibration at 1252 cm^{-1} may be assigned to deformation vibration of C=O and stretching vibration of –OH of carboxylic acids and phenols. The intense band at 1042 cm^{-1} is related to the C–OH stretching vibration of alcoholic groups and carboxylic acids. The presence of sulfur groups in spectrum the xCC has been identified by the appearance of new peaks at 600, 1025, and 1159 cm^{-1} corresponding to C–S, C=S, and S–C–S. The peak at 1252 cm^{-1}, present in the spectrum of CC, was disappeared in spectrum of xCC, which may indicate that this group can be involved in the synthesis process of xanthate groups.

The SEM image and EDX analysis of xCC and loaded xCC with Cr(III) ions and MB are shown in Fig. 2. The SEM images (Fig. 2) show a porous morphology of unloaded and loaded Cr(III) ions material; the external surface is full of cavities with pores of different sizes and shapes (irregular tubular structure with cavity 10–30 μm in diameter for xCC). The presence of macropores increases possibility of penetration and sorption of Cr(III) ions and MB through xCC with the diffusion.

EDX analysis and elemental composition before and after sorption of Cr(III) ions on xCC are shown in Fig. 2. The elemental composition of xCC is in accordance with the chemical composition of lignocellulosic materials. The presence of sulfur peaks in EDX spectra of xCC indicated emergence of xanthate group on the sorbent. After loading of Cr(III) ions, the presence of characteristic signal for Cr in EDX spectra (Fig. 2b) was observed, thus suggesting that the Cr was sorbed onto xCC. The percentage of Na in xCC was visibly changed after the sorption of the Cr(III) ions which indicates that ion exchange probably existed in the sorption process.

Physical characteristics and elemental analysis of xCC are summarized in Table 1.

Effect of initial pH on Cr(III) ions and MB removal

The results of Cr(III) ions and MB sorption onto xCC at different pH values are illustrated in Fig. 3. The figure shows that at pH 2, the sorption capacity of Cr(III) ions on xCC was minimum, after that large increase of sorption capacity of Cr(III) ions occurs, and at pH 5, the removal was maximum. Similar conclusion was found for Cr(III) ions sorption onto aerobic granules (Yao et al. 2009). It is well known that the increase of pH solution reduces the competition between the H^+ and the Cr(III) ions, favoring sorption at high pH, i.e., as pH rises sorbent surface becomes more negative and enables unobstructed binding. The biosorption of MB on xCC is low in acidic medium and with the increase of pH,

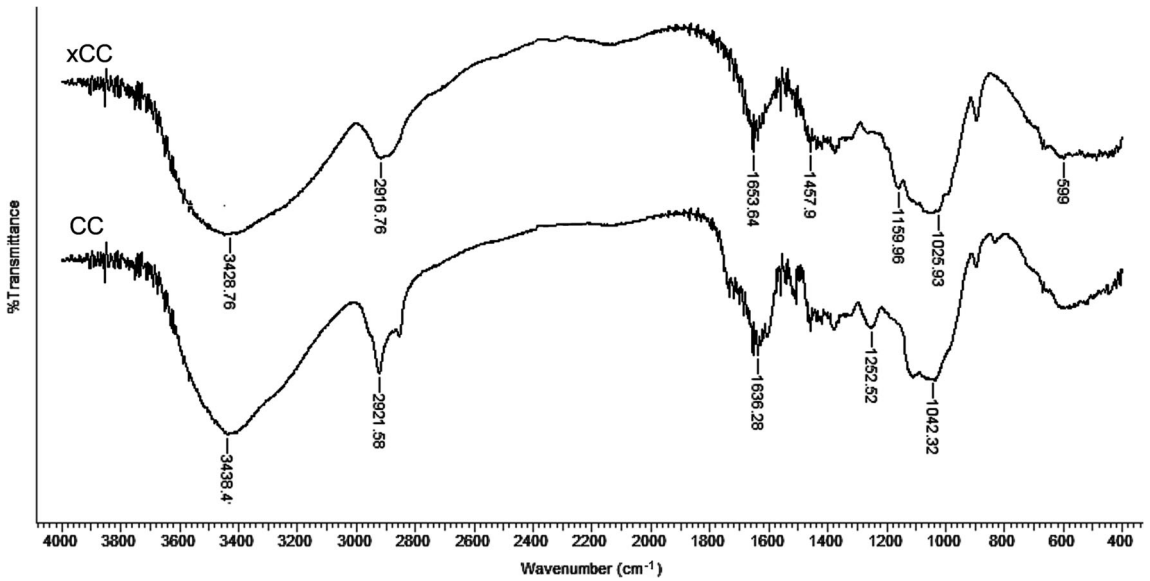

Fig. 1 FTIR spectra of CC and xCC

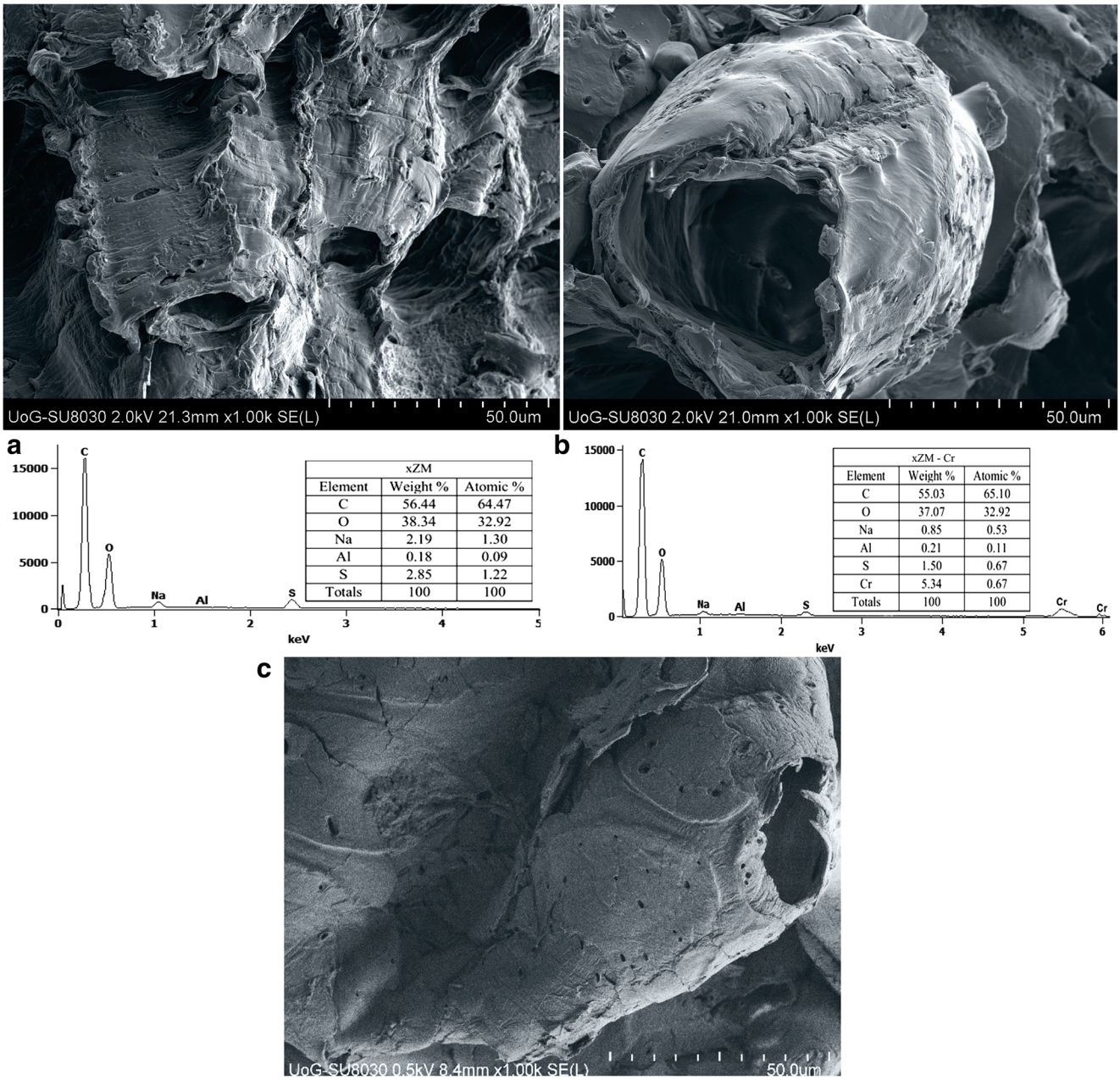

Fig. 2 **a** The morphology surface and EDX analysis of xCC. **b** Cr(III) ions loaded on xCC. **c** The morphology surface of MB loaded on xCC

the sorption capacity for MB increases. When solution pH was increased up to 5, the sorption of MB rapidly increases, whereas in the range from 5 to 8, there was only slightly increase by pH. Therefore, pH 5 was chosen to carry out further investigation which is in accordance with the obtained values for pHpzc (Table 1). The sorption efficiency at pH values below pHpzc is high, because of the presence of strong acid xanthate groups, which are not protonated in applied conditions. These negative groups have high affinity for the binding of positively charged metal ions, even at a relatively low pH, probably by means of the ion exchange mechanism. At pH values about pHpzc, the surface of the sorbent becomes negatively charged and the surface will be such so as to enhances the sorption with Cr(III) ions and MB as a cationic dye with xCC (Guiza 2017).

Effect of sorbent dosage on Cr(III) ions and MB removal

The effects of sorbent dose on removal efficiency and the removal efficiency per unit weight of sorbent (RE %/dose) have also been investigated (Fig. 4) to define optimal sorbent

Table 1 Physical characteristics and elemental analysis of xCC

Characteristics	xCC
Moisture (%)	5.36
Ash (%)	0.95
Bulk density (kg m^{-3})	275.75
pHpzc	7.19
CEC (cmol(+) kg^{-1})	20.2
C (%)	47.17
O (%)	44.09
H (%)	6.18
N (%)	0.01
S (%)	2.55

dose. It was examined by varying the amount of xCC from 0.5 to 8.0 g dm^{-3}, while keeping other parameters constant. The results showed that with increase of sorbent dose from 0.5 to 8.0 g dm^{-3}, removal efficiency on xCC increases from 10 to 89% for Cr(III) ions and from 26 to 60% for MB. With increase of sorbent dose, this increases surface area and the availability of sorption sites. The biggest changes were noted with increase of sorbent dose from 0.5 to 4.0 g dm^{-3} when removal efficiency of Cr(III) ions increases from 10 to 83%. The biggest changes were in the range of sorbent dose from 0.5 to 1.0 g dm^{-3} when removal efficiency of MB increases from 25 to 51%. A further increase in biosorbent dosage did not cause a significant improvement in sorption. There are many factors which can contribute to this phenomenon. Probably the most important is fact that some sorption sites remain unoccupied because of the overlapping or aggregation of biosorbent particles (decreasing in total sorbent surface area) (El Nemr et al. 2015; Hafshejani et al. 2015).

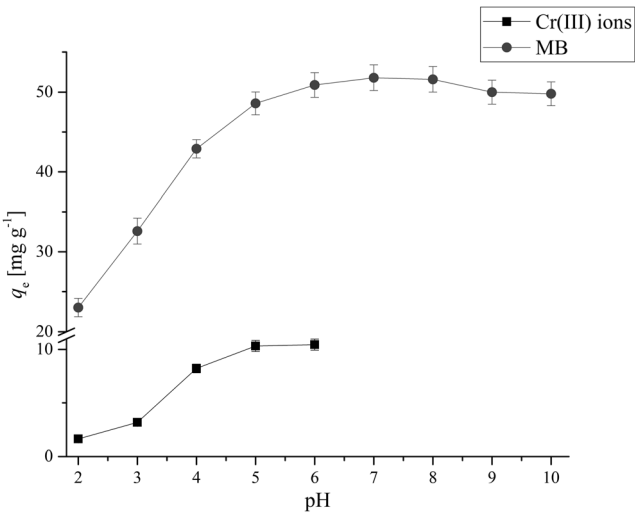

Fig. 3 Effect of pH on the removal efficiency of Cr(III) ions and MB onto xCC. c_0 [Cr(III)] = 50.0 mg dm^{-3} and c_0 [MB] = 100 mg dm^{-3} MB, sorbent dose 4.0 g dm^{-3} for removal Cr(III) ions and 1.0 g dm^{-3} for removal MB, temperature 20.0 ± 0.2 °C, and stirring speed 200 rpm

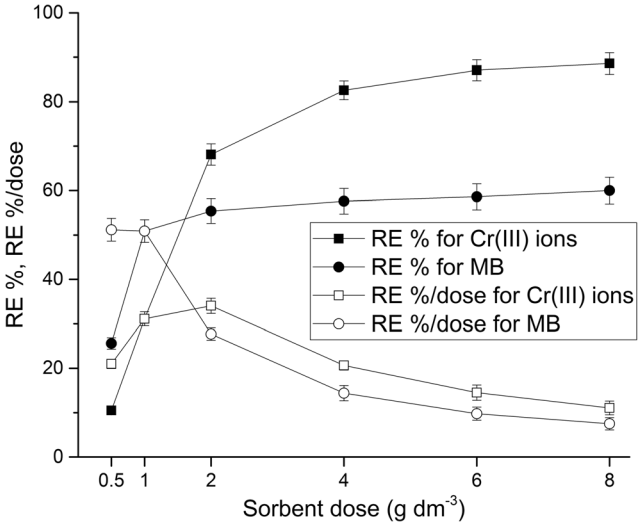

Fig. 4 Effect of sorbent dosage on the removal efficiency and the removal efficiency per unit weight of sorbent of Cr(III) ions and MB onto xCC. c_0 [Cr(III)] = 50.0 mg dm^{-3} and c_0 [MB] = 100 mg dm^{-3} MB, pH 5, temperature 20.0 ± 0.2 °C, and stirring speed 200 rpm

However, with increasing sorbent dosage from 0.5 to 8.0 g dm^{-3} (Fig. 4), the removal efficiency of Cr(III) ions and MB per unit weight of sorbent (RE %/dose) decreased. In the case of Cr(III) ions for dose from 0.5 to 2.0 g dm^{-3} and for MB from dose 0.5 to 1.0 g dm^{-3}, value of RE %/dose is almost constant, with further decreasing. By comparison of presented results of change of RE % and RE %/dose, the dose of 4 g dm^{-3} for removal Cr(III) ions and 1 g dm^{-3} for removal MB was picked as optimal for all experiments.

Effect of particle size on Cr(III) ions and MB removal

The experiments were carried out for five different particle sizes of xCC: 0.1–0.4, 0.4–0.8, 0.8–1.25, 1.25–2.5, and 2.5–4.0 (shown in Fig. 5). With increasing particle size from 0.1–0.4 to 2.5–4.0, removal efficiency decreased from 83.5 to 72.5% for removal Cr(III) ions and from 52.9 to 47.6% for removal MB onto xCC. In accordance with literature, reduce of particle size leads to increasing of effective surface area (Singh et al. 2008; Gilbert et al. 2011). The particle size 0.8–1.25 mm was selected for further experiments due to their high removal efficiency for Cr(III) ions, while smaller particles, besides insignificant better removal efficiency, were not suitable because it was more difficult to remove them from dispersion.

Effect of stirring speed on Cr(III) ions and MB removal

The effect of stirring speed on removal efficiency of Cr(III) ions and MB was studied in the range from 100 to 600 rpm (Fig. 6). Optimal value of removal efficiency for Cr(III) ions and MB on xCC was obtained for a stirring speed of 200 rpm. Increasing stirring rate increases probability of collision

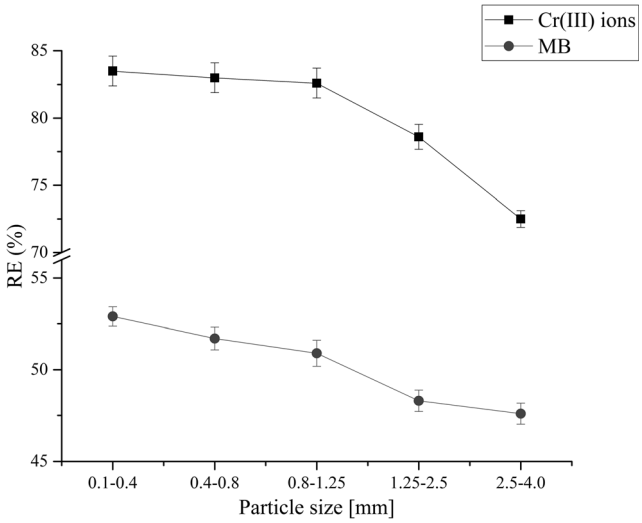

Fig. 5 Effect of particle size on the removal efficiency of Cr(III) ions onto xCC. c_0 [Cr(III)] = 50.0 mg dm^{-3} and c_0 [MB] = 100 mg dm^{-3} MB, sorbent dose 4.0 g dm^{-3} for removal Cr(III) ions and 1.0 g dm^{-3} for removal MB, temperature 20.0 ± 0.2 °C, and stirring speed 200 rpm

between Cr(III) ions and sorbent particles, i.e., film boundary layer thickness, surrounding the sorbent particles decreases which results in a reduction in surface film resistance. However, at high stirring speed, the suspension was no longer homogenous and vortex phenomena can occur (Selatnia et al. 2004). This is also supported by literature.

Kinetic study

In order to investigate the biosorption mechanism of Cr(III) ions and MB on xCC and rate-controlling steps, a kinetic investigation was conducted. The kinetic sorption constants were determined in terms of pseudo-first-order, pseudo-second-order, intraparticle diffusion, and Chrastil's kinetic models.

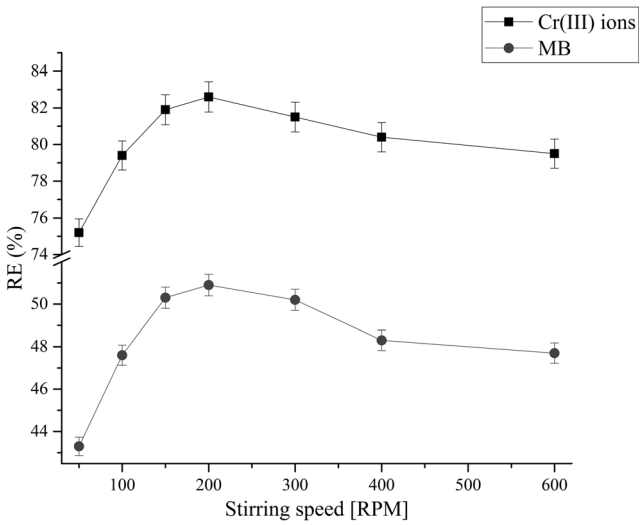

Fig. 6 Effect of stirring speed on the removal efficiency of Cr(III) ions onto xCC. c_0 [Cr(III)] = 50.0 mg dm^{-3} and c_0 [MB] = 100 mg dm^{-3} MB, sorbent dose 4.0 g dm^{-3} for removal Cr(III) ions and 1.0 g dm^{-3} for removal MB, and temperature 20.0 ± 0.2 °C

The first-order rate expression of Lagergren states that the rate of occupation of sorption sites should be proportional to the number of unoccupied sites (Meseguer et al. 2016). The non-linear form of this equation is as follows

$$q_t = q_e\left(1-e^{-k_1 t}\right) \tag{3}$$

where q_e (mg g^{-1}) is the mass of metal ions sorbed at equilibrium, q_t (mg g^{-1}) is the mass of metal sorbed at time t, and k_1 (min^{-1}) is the pseudo-first-order reaction rate equilibrium constant.

The pseudo-second-order equation is also based on the sorption capacity of the solid phase and non-linear form of equation is expressed as follows (Deniz and Kepekci 2017)

$$q_t = \frac{k_2 q_e^2 t}{1 + k_2 q_e t} \tag{4}$$

where k_2 (g mg^{-1} min^{-1}) is the rate constant of second-order sorption.

Intraparticle diffusion equation was introduced to indicate the behavior of intraparticle diffusion as the rate-limiting step in the biosorption (Altenor et al. 2009). The intraparticle equation can be described as follows

$$q_t = K_{\mathrm{ID}} t^{\frac{1}{2}} + C \tag{5}$$

where K_{ID} (mg g^{-1} min$^{-1/2}$) is the internal diffusion coefficient, C is the intercept, and the foregoing parameters can be determined from a plot of q_t versus $t^{1/2}$ (values of intercept give an idea about the thickness of boundary layer).

Finally Chrastil's model is analyzed and Chrastil's equation can be described as

$$q_t = q_e\left(1-e^{-k_c A_0 t}\right)^n \tag{6}$$

where k_c is a rate constant (dm^3 g^{-1} min^{-1}), which depends on diffusion coefficients and sorption capacity of biosorbent, A_0 is dose of biosorbent (g dm^{-3}), and n is a heterogeneous structural diffusion resistance constant, which can be ranged from 0 to 1. When diffusion resistance is small, n tends to 1 and the reaction is of first order. If the system is strongly limited by diffusion resistance, n is small. In addition, when $n > 1$, a consecutive reaction order may be expected (Carrillo et al. 2005; Chrastil 1990).

Calculated correlation coefficients and kinetics parameters are shown in Tables 2 and 3. The coefficient of correlation values for sorption Cr(III) ions on xCC was for pseudo-first order in the range from 0.954 to 0.985 and for pseudo-second-order kinetic from 0.990 to 1.000, respectively (Table 2). It is clear that determination coefficients (r^2) for pseudo-second-order model are the largest. The sorption capacities calculated

Table 2 The values of kinetic parameters for applied kinetic models for sorption Cr(III) ions on xCC (sorbent dose 1.0 g dm^{-3}, temperature 20.0 ± 0.2 °C)

Cr(III)ions (mg dm^{-3})	10	20	50	100	200	400
q_e^{exp}	2.285	4.600	10.325	14.100	16.450	17.062
Pseudo-first order						
k_1	0.145	0.142	0.153	0.197	0.184	0.166
q_e^{cal}	2.228	4.428	9.981	13.481	15.525	16.198
r^2	0.985	0.985	0.975	0.962	0.954	0.958
Pseudo-second order						
k_2	0.224	0.215	0.244	0.328	0.299	0.269
q_e^{cal}	2.380	4.744	10.618	14.255	16.469	17.211
r^2	0.998	1.000	0.995	0.994	0.990	0.991
Chrastil's model						
q_e	2.270	4.519	10.240	13.953	16.190	16.847
N	0.600	0.591	0.495	0.419	0.389	0.407
k_c	0.021	0.020	0.017	0.017	0.014	0.014
r^2	0.997	0.996	0.999	0.997	0.994	0.997
Intraparticle diffusion model						
K_{id1}	0.567	1.100	2.439	3.760	4.149	4.171
C_1	−0.046	−0.082	0.081	0.188	0.274	0.250
r^2	0.974	0.978	0.996	0.990	0.983	0.986
K_{id2}	0.185	0.318	0.678	0.799	0.805	0.985
C_2	1.059	2.300	5.511	8.335	9.850	9.414
r^2	0.960	0.872	0.869	0.999	0.991	0.949

by pseudo-second-order model are close to those determined by experiments, so that this model certainly describes the sorption kinetics of Cr(III) onto xCC. Similar kinetic results have been reported by other researchers (Elabbas et al. 2016;

Table 3 The values of kinetic parameters for applied kinetic models for sorption MB on xCC (sorbent dose 1.0 g dm^{-3}, temperature 20.0 ± 0.2 °C)

MB (mg dm^{-3})	100	150	200	250	400
q_e^{exp}	51.500	65.300	73.956	79.580	82.320
Pseudo-first order					
k_1	0.047	0.076	0.093	0.086	0.053
q_e^{cal}	50.259	61.496	70.044	75.184	79.581
r^2	0.995	0.980	0.984	0.982	0.992
Pseudo-second order					
k_2	0.047	0.098	0.127	0.116	0.063
q_e^{cal}	58.601	68.775	77.149	83.206	91.618
r^2	0.995	0.999	1.000	0.999	0.998
Chrastil's model					
q_e	51.479	63.786	71.875	77.503	81.949
n	0.763	0.611	0.629	0.611	0.703
k_c	0.034	0.040	0.054	0.047	0.034
r^2	1.000	0.994	0.996	0.996	0.999
Intraparticle diffusion model					
K_{id1}	6.858	9.311	11.062	11.587	11.196
C_1	−2.053	0.786	2.444	2.216	−1.948
r^2	0.988	0.959	0.949	0.956	0.991
K_{id2}	2.823	2.535	1.991	2.568	3.879
C_2	23.168	38.028	52.223	52.009	42.489
r^2	0.911	1.000	0.957	0.940	0.984

Iftikhar et al. 2009). In Table 3, the values of coefficients of correlation for the sorption of MB onto xCC are shown, which show that the pseudo-first and pseudo-second models have a good agreement with experimental data. Therefore, it can be concluded that pseudo-second-order model something better can describe kinetics sorption for MB onto xCC. The sorption capacities calculated by the pseudo-first and pseudo-second model are close to those determined by experiments.

Figure 7a, b shows the plot of amount of Cr(III) ions/MB sorbed, q_t versus $t^{1/2}$, for Cr(III) ions/xCC system and the MB/xCC system. The kinetic data for all initial Cr(III) and MB concentrations were tested, and shows that the plot has three linear segments, initially curved portion, which suggest film diffusion and the subsequent linear portion attribute to the intraparticle diffusion. The second region corresponds to the gradual uptake, which reflects at the intraparticle diffusion as the rate-limiting step and increase in initial concentration will produce a higher concentration of gradient, which will cause faster diffusion and sorption. The final plateau indicates the equilibrium uptake which implicates that the intraparticle diffusion is not the only rate-controlling step.

The Chrastil's model, based on Eq. 6, was applied to all concentrations (non-linear regression analysis) and was shown in Tables 2 and 3. The coefficients of determinations in all cases were very high ($r^2 > 0.99$). The results obtained for the diffusion resistance coefficient values were in the range from 0.389 to 0.600 for removal of Cr(III) ions onto xCC and from 0.611 to 0.763 for removal MB onto xCC. This indicates that the sorption process of Cr(III) ions and MB on xCC is significantly limited by diffusion resistance. Lower values of n and higher values for k_c at Cr(III) ions sorption indicate that the system is strongly limited by diffusion resistance probably due to the formation of trivalent chromium hydroxy species at pH >3.5 (Karaoglu et al. 2010).

Sorption isotherms

Several isotherm models have been used in the literature to describe the sorption equilibrium data, such as Langmuir (Koutahzadeh et al. 2013; Park and Chon 2016), Freundlich (Puchana-Rosero et al. 2016), Sips (Limousy et al. 2016), Hill (Woitovich Valetti and Picó 2016), Toth (Rafati et al. 2016), Khan (Khan et al. 1997), and Brouers–Sotolongo (Altenor et al. 2009). The non-linear forms of the Langmuir (Eq. 7), Freundlich (Eq. 8), Sips (Eq. 9), Hill (Eq. 10), Toth (Eq. 11), Khan (Eq. 12), and Brouers–Sotolongo (Eq. 13) models are represented as follows

$$q_e = \frac{q_m K_L c_e}{1 + K_L c_e} \tag{7}$$

$$q_e = K_F c_e^{\frac{1}{n}} \tag{8}$$

$$q_e = \frac{q_m (b_S c_e)^n}{1 + (b_S c_e)^n} \tag{9}$$

$$q_e = \frac{q_H {c_e}^{n_H}}{K_D + {c_e}^{n_H}} \tag{10}$$

$$q_e = \frac{K_T c_e}{(a_T + c_e)^{1/t}} \tag{11}$$

$$q_e = \frac{a_S b_K c_e}{(1 + b_K c_e)^{a_K}} \tag{12}$$

$$q_e = q_m \left(1 - e^{\left(-K_W C_e^{\alpha}\right)}\right) \tag{13}$$

where q_e is the amount of heavy metal ions sorbed (mg g^{-1}) by the sorbent at equilibrium time; c_e is the concentration (mg dm^{-3}) of metal ions and dye at equilibrium time in solution; q_m is the maximum sorption capacity of sorbent (mg g^{-1}); K_L is Langmuir constant related to the energy of sorption

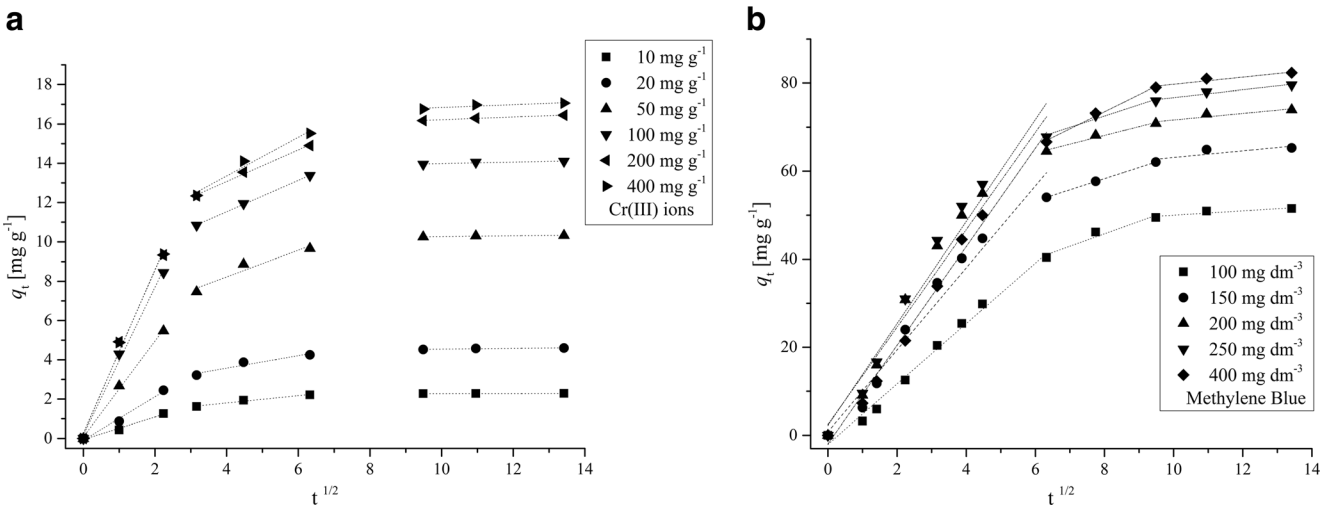

Fig. 7 **a** Intraparticle diffusion plot for Cr(III) ions sorption on xCC (Sorbent dose 4.0 g dm^{-3}, pH 5.0, stirring speed 200 rpm, and temperature 20.0 ± 0.2 °C). **b** Intraparticle diffusion plot for MB sorption on xCC (sorbent dose 1.0 g dm^{-3}, pH 5.0, stirring speed 200 rpm, and temperature 20.0 ± 0.2 °C)

Table 4 Parameters for Langmuir, Freundlich, Sips, Hill, Toth, Khan, and Brouers–Sotolongo (B–S) isotherm models of Cr(III) ions sorption on xCC

Isotherm	Calculated parameters							
Langmuir at 10 °C	q_m	16.491	K_L	0.158			r^2	0.996
Langmuir at 20 °C		16.807		0.191				0.989
Langmuir at 30 °C		16.635		0.210				0.992
Langmuir at 40 °C		17.130		0.242				0.987
Freundlich at 10 °C	K_F	4.885	n	4.394				0.846
Freundlich at 20 °C		5.236		4.523				0.863
Freundlich at 30 °C		5.394		4.659				0.873
Freundlich at 40 °C		5.960		4.959				0.843
Sips at 10 °C	q_m	16.699	b_S	0.151	n_S	0.944		0.994
Sips at 20 °C		17.523		0.162		0.835		0.993
Sips at 30 °C		17.529		0.173		0.793		0.998
Sips at 40 °C		17.876		0.212		0.803		0.994
Hill at 10 °C	q_H	16.696	n_H	0.945	K_D	5.967		0.994
Hill at 20 °C		17.520		0.835		4.571		0.993
Hill at 30 °C		17.528		0.793		4.029		0.998
Hill at 40 °C		17.877		0.803		3.476		0.994
Toth at 10 °C	K_T	13.686	a_T	5.0872	t	1.036		0.996
Toth at 20 °C		12.405		3.460		1.062		0.996
Toth at 30 °C		11.976		2.921		1.067		0.999
Toth at 40 °C		13.977		2.970		1.040		0.987
Khan at 10 °C	q_S	14.497	b_K	0.196	a_K	0.965		0.996
Khan at 20 °C		13.332		0.289		0.942		0.996
Khan at 30 °C		12.811		0.342		0.937		0.999
Khan at 40 °C		14.566		0.337		0.961		0.987
B–S at 10 °C	q_m	16.064	K_W	0.194	α	0.660		0.979
B–S at 20 °C		16.717		0.232		0.595		0.981
B–S at 30 °C		16.616		0.254		0.575		0.988
B–S at 40 °C		16.923		0.271		0.613		0.997

(dm^{-3} mg^{-1}), K_F is Freundlich equilibrium constant (mg g^{-1}) (dm^3 $mg^{-1})^{1/n}$ and n (g dm^{-3}) is exponent; b_S (dm^{-3} mg^{-1}) in Sips model is the affinity constant for sorption; q_H is Hill isotherm maximum uptake saturation (mg dm^{-3}); n_H is Hill cooperativity coefficient of the binding interaction; and K_D is Hill constant in equitation of Hill model. K_T is Toth isotherm constant (mg g^{-1}); a_T is Toth isotherm constant (dm^3 mg^{-1}); t is Toth isotherm constant; q_S is theoretical isotherm saturation capacity (mg g^{-1}); b_K is Khan isotherm model constant; a_K is Khan isotherm model exponent; K_W is Brouers–Sotolongo isotherm constant ((mg g^{-1}) (dm^3 mg^{-1})$1/\alpha$); and α is Brouers–Sotolongo model exponent.

The differences between all these models are reflected in the homogeneous or heterogeneous sorption, presence or absence of a maximum sorption monolayer, and the number of parameters to fit. The isotherm models were fitted with experimental data by non-linear modeling using Origin Pro 2016, and calculated results are shown in Tables 4 and 5. The isotherm models have been used to investigate the sorption equilibrium between the metal and dye solution and the solid phase (xCC). As it can be seen in Tables 4 and 5, the coefficients of determinations (r^2) obtained for Langmuir isotherm model in all cases were high ($r^2 > 0.97$) for sorption Cr(III) ions and MB on xCC at all temperatures, but not the greatest. However, values q_m fitted by Langmuir isotherm model were closest to the experimentally obtained q_m values at temperatures 10, 20, and 30 °C for sorption Cr(III) ions on xCC. At temperature of 40 °C, the coefficients of determinations obtained for Sips and Hill isotherm models are greater than the coefficients of determinations obtained for Langmuir model and values q_m fitted by Sips and Hill isotherm model were closest to the experimentally obtained q_m value for sorption Cr(III) ions on xCC. The maximum sorption capacity predicted by the Langmuir (16.49, 16.81, 16.63, and 17.13 mg g^{-1} for temperatures 10, 20, 30, and 40 °C, respectively) and Sips and Hill (16.70, 17.52, 17.53, and 17.88 mg g^{-1} for temperatures 10, 20, 30, and 40 °C, respectively) isotherms were approximately same as the experimentally obtained values (16.5, 17.06, 17.03, and 17.30 mg g^{-1} for temperatures 10, 20, 30, and 40 °C, respectively) or sorption Cr(III) ions onto xCC.

Table 5 Parameters for Langmuir, Freundlich, Sips, Hill, Toth, Khan, and Brouers–Sotolongo isotherm models of MB sorption on xCC

Isotherm	Calculated parameters							
Langmuir at 10 °C	q_m	91.857	K_L	0.025			r^2	0.973
Langmuir at 20 °C		94.791		0.026				0.971
Langmuir at 30 °C		93.293		0.029				0.970
Langmuir at 40 °C		93.535		0.031				0.971
Freundlich at 10 °C	K_F	21.882	n	4.310				0.837
Freundlich at 20 °C		23.462		4.410				0.832
Freundlich at 30 °C		25.300		4.703				0.825
Freundlich at 40 °C		26.940		4.910				0.828
Sips at 10 °C	q_m	83.275	b_S	0.025	n_S	1.523		0.996
Sips at 20 °C		86.779		0.026		1.462		0.987
Sips at 30 °C		85.896		0.028		1.468		0.987
Sips at 40 °C		87.297		0.030		1.386		0.980
Hill at 10 °C	q_H	83.275	n_H	1.523	K_D	274.820		0.996
Hill at 20 °C		86.781		1.462		202.973		0.987
Hill at 30 °C		85.896		1.468		186.799		0.987
Hill at 40 °C		87.300		1.385		125.600		0.980
Toth at 10 °C	K_T	576.808	a_T	92.113	t	0.777		1.000
Toth at 20 °C		528.343		85.218		0.787		0.996
Toth at 30 °C		407.167		73.438		0.811		0.995
Toth at 40 °C		309.146		62.480		0.840		0.991
Khan at 10 °C	q_S	157.455	b_K	0.011	a_K	1.287		1.000
Khan at 20 °C		159.080		0.012		1.270		0.996
Khan at 30 °C		149.297		0.014		1.233		0.995
Khan at 40 °C		140.304		0.016		1.191		0.991
B–S at 10 °C	q_m	80.092	K_W	0.027	α	0.908		0.999
B–S at 20 °C		83.254		0.031		0.883		0.995
B–S at 30 °C		82.756		0.036		0.864		0.994
B–S at 40 °C		83.891		0.044		0.823		0.991

From Table 5, it was observed that the Brouers–Sotolongo isotherm model beside Sips and Hill models gives the best fit to the experimental data for sorption MB on xCC, which indicates the presence of active sites with heterogeneous sorption interactions. It can be inferred that the sorption environment in xCC material was heterogeneous based on α (being related to the heterogeneity $\alpha < 1$).The maximum sorption capacity predicted by Brouers–Sotolongo (80.09, 83.25, 82.76, and 83.89 mg g^{-1} for temperatures 10, 20, 30, and 40 °C, respectively) and Sips and Hill (83.27, 86.78, 85.90, and 87.30 mg g^{-1} for temperatures 10, 20, 30, and 40 °C, respectively) isotherm models were approximately same as the experimentally obtained values (79.5, 82.32, 81.90, and 82.8 mg g^{-1} for temperatures 10, 20, 30, and 40 °C, respectively) for sorption MB onto xCC. Considering the q_m values, Brouers–Sotolongo equation is the most adapted for fitting sorption isotherms of MB on the xCC.

Taking into consideration values q_m and r^2 obtained from non-linear regression of Langmuir isotherm models, sorption of Cr(III) ions and MB on xCC occurs on a homogeneous surface by monolayer sorption without any interaction between sorbed ions, which indicates that the chemical mechanism of sorption probably prevails. However, the fact is that Sips isotherm model (hybrid of Langmuir and Freundlich isotherm models that is based on the theory of a homogenous–heterogeneous sorbent surface) in good agreement with experimental data indicates that in high sorbate concentrations, this predicts monolayer sorption onto surface of sorbent like at the Langmuir isotherm, while at low sorbate concentration, it follows Freundlich isotherm. Hill model, which describes the binding of different species onto homogeneous substrates, i.e., ability ligand binding at one site on the macromolecule, may influence different binding sites on same macromolecule, while Brouers–Sotolongo isotherm was specifically developed for the complex and heterogeneous systems, making it suitable to describe sorption phenomena involving sorbing materials with different chemical and structural characteristics which is precisely the case in this study. The Langmuir sorption model deviates primarily because it fails to account for the surface roughness of the sorbate and multi-layered

sorption phenomenon. The results show that the Cr(III) ions and MB sorption onto xCC is a complex process because of heterogeneous surface as a consequence of differences in size and shape of pores, cracks and pits and different functional groups (xanthate, carboxylic, hydroxyl etc.) so sorption between Cr(III) and MB on xCC occurs via different possible interactions mainly electrostatic attraction, ion exchange, and complexation. Electrostatic interactions are clearly involved in Cr(III) ions and MB sorption mechanism. The acidic groups such as xanthate and carboxylic groups favor sorption due to electrostatic interactions between the Cr(III) ions and MB molecules and the deprotonated xanthate and carboxylic groups. Furthermore, ion exchange is an important concept in biosorption mechanisms; the ion exchange reaction occurs between light metals, such as Na^+, which are released upon binding of a cation on xCC.

The coefficients of determinations for Freundlich, Toth, and Khan isotherm models are relatively equal to or less compared to those of Langmuir, Sips, Hill, and Brouers–Sotolongo models. The experimental q_m values did not agree with the calculated sorption capacity values obtained from the Freundlich, Toth, and Khan isotherm models. From the analysis of all the isotherms and the knowledge of the most important parameters (q_m and r^2), the comparison of tested models for the description of sorption equilibrium isotherms on xCC is as follows: Langmuir ≥ Sips ≥ Hill > Brouers–Sotolongo > Toth ≥ Khan > Freundlich for Cr(III) ions and Brouers–Sotolongo ≥ Sips ≥ Hill > Langmuir > Toth ≥ Khan > Freundlich for MB. The results show that maximum sorption capacity calculated for non-linear models increased as the temperature increases and at temperature of 40 °C reaches the maximum value and amounts 17.13 mg g^{-1} (Langmuir) for sorption Cr(III) ions and 83.89 mg g^{-1} (Brouers–Sotolongo) for sorption MB on xCC, because the increase rate of diffusion of the sorbate molecules across the external boundary layer and in internal pores of the sorbent particles is the result of the reduced viscosity of the solution (micropores favor Cr(III) ions sorption, while mesopores favor MB sorption). In the similar conditions, at 25 °C, basic material (non-modified corn cob) shows much smaller sorption capacity (3.22 mg g^{-1} for Cr(III) and 16.21 mg g^{-1} for MB), which confirms significance of chemical modification. Values for K_L and K_W increase with increasing temperature from 10 to 40 °C that indicates that the Cr(III) ions and MP are favorably sorbed by xCC at higher temperatures, i.e., the sorption process is endothermic. The separation factor (R_L) value determined from the Langmuir isotherm indicated that Cr(III) ions and MB sorption onto xCC were in favorable region ($R_L < 1$). The decrease in R_L with an increase in the initial concentration indicates that the sorption is more favorable at high concentrations. The values of n_H for MP were >1, which indicated the fact that the interaction of binding between MP and xCC was in the form of positive cooperativity.

Biosorption thermodynamics

The thermodynamic parameters, including the free energy change ($\Delta G°$, kJ mol^{-1}), enthalpy change ($\Delta H°$, kJ mol^{-1}), and entropy change ($\Delta S°$, J mol^{-1}), can be estimated using equilibrium constant values as a function of temperature. The free energy change of the sorption reaction is given by the following equation (Kesraoui et al. 2016)

$$\Delta \mathring{G} = -RT\ln K \tag{14}$$

where $\Delta G°$ is standard free energy change, J; R the universal gas constant, 8.314 J mol^{-1} K^{-1}; T the absolute temperature, K; and K is the equilibrium constant obtained from the Langmuir model (K_L) for sorption Cr(III) ions and Brouers–Sotolongo model (K_W) for sorption MB on xCC.

The free energy change indicates the degree of spontaneity of the sorption process and a higher negative value reflects more energetically favorable sorption process (Özer et al. 2004). The equilibrium constant may be expressed in terms of entropy change and enthalpy change as a function of temperature as follows (the van't Hoff equation)

$$\Delta G = \frac{\Delta \mathring{S}}{R} - \frac{\Delta \mathring{H}}{RT} \tag{15}$$

According this equation, the effect of temperature on the equilibrium constant K is determined by the sign of $\Delta H°$. Thus, when $\Delta H°$ is positive, i.e., when the sorption is endothermic, increase of temperature results in increase of K. Conversely, when $\Delta H°$ is negative, i.e., when the sorption is exothermic, increase of temperature causes decrease of K. This implies shifting of the sorption equilibrium to the left. The other useful parameters are $\Delta H°$ and $\Delta S°$, and they are given by the following

$$\Delta G = \Delta \mathring{H} - T\Delta \mathring{S} \tag{16}$$

The standards enthalpy and entropy changes are determined from the slope and intercept of the plot of ln K versus $1000/T$ (The plot of ln K versus $1000/T$ is given in supplementary data Fig. S1), respectively, and are summarized in Table 6.

The r^2 values of the linear fitting experimental data were >0.98, which indicates the values of enthalpy and entropy change calculated for sorption Cr(III) ions and MB on xCC are fairly confident. The values K increase by increasing of temperature, suggesting that the sorption process is endothermic, and the sorption capacity increases with increasing of temperature. Increase of temperatures leads to increasing of the sorption capacity, which may be attributed to the enlargement of pore size and activation of the sorbent surface. The negative

Table 6 Thermodynamic parameters for the sorption of Cr(III) ions and MB onto xCC

	T (°C)	q_m (mg g^{-1})	Ln K	r^2 (ln K versus 1/T)	$\Delta G°$ (kJ mol^{-1})	$\Delta H°$ (kJ mol^{-1})	$\Delta S°$ (J mol^{-1})
Cr(III) ions	10	16.491	9.01439	0.982	−21.22	10.19	111.03
	20	16.807	9.20387		−22.43		
	30	16.635	9.30081		−23.44		
	40	17.130	9.44185		−24.58		
MB	10	80.092	9.06560	0.973	−21.34	11.63	116.31
	20	83.254	9.20105		−22.42		
	30	82.756	9.34081		−23.54		
	40	83.891	9.54705		−24.86		

$\Delta G°$ value at all temperatures points out that sorption processes were spontaneous nature and feasible; by increasing the temperature, the value of $\Delta G°$ becomes more negative, suggesting that higher temperature makes the sorption favorable (Li et al. 2015). The positive values of $\Delta H°$ (about 10 kJ mol^{-1}) show that the nature of sorption is endothermic and suggest that the sorption is physico-chemical process (Elabbas et al. 2016). The positive values of $\Delta S°$ also indicate the possibility of some structural changes, increase in disorder of system's interface, and may indicate that ion replacement reaction is taking place. The positive value of $\Delta S°$ suggests that the process is enthalpy driven. Similar results were also reported by other researchers (Sawalha et al. 2006; Elabbas et al. 2016).

Removal of Cr(III) ions and MB from wastewater

The removal efficiency of Cr(III) ions and MB, as well as amount of xanthated biosorbent, could be predicted based on equilibrium data and mathematical tools for results interpretation. For predicting performances of sorption based on sorption isotherms (Langmuir and Brouers–Sotolongo), two equations were used (Eqs. 17 and 18), obtained by combining Eq. 1 with Eqs. 7 and 9.

$$\frac{m}{V}=\frac{c_0-c_t}{q_m}=\frac{c_0-c_t}{\frac{q_m K_L c_e}{1+K_L c_e}} \tag{17}$$

$$\frac{m}{V}=\frac{c_0-c_t}{q_m}=\frac{c_0-c_t}{q_m\left(1-e^{\left(-K_W C_e^{\alpha}\right)}\right)} \tag{18}$$

The plots obtained from Eqs. 17 and 18 (Fig. 8a, b) indicate the predicted amount of xCC required for removing Cr(III) ions and MB from solutions (initial concentration of Cr(III) ions was 20 mg dm^{-3} and of MB was 100 mg dm^{-3}) to the extent of 80–99% removal for different solution volumes (1–5 dm^3).

For example, from Fig. 8, it can be seen that for removal efficiency of 99% for volumes 1, 2, 3, 4, and 5 dm^{-3}, the amounts of xCC were 1.18, 2.36, 3.53, 4.71, and 5.89, and 1.19, 2.38, 3.57, 4.76, and 5.95 g for Cr(III) and MB solutions, respectively. However, in the experimental results obtained with the same amount of sorbent, there was a slightly higher removal efficiency, on average about 5%.

In the chrome plating industry, the plated metal parts are rinsed with water in one or more rinsing baths. In this study, treatment of effluent from rinsing baths of chrome plating line is carried out by continuous circulating of effluent through the column. After saturation, the column would be changed or there would be second column with by-bass which enable continuous process. The concentration of Cr(III) ions in tanks must be reduced to the level in accordance with environmental regulations for various types of water and industrial wastewaters, before discharging. This wastewater from chrome plating industry contains chrome in the range from 80 to 160 mg dm^{-3}. In the case of this study, wastewater was from chrome plating company Galpres, Leskovac, which contains Cr in concentration of 114 mg dm^{-3}. Hexavalent chromium was reduced to Cr(III) by using chemical reducing agents such as sodium bisulfite at pH about 2.8 (pH was adjusted to the desired pH with sulfuric acid). In the next step, $Ca(OH)_2$ was added for Cr(III) precipitation as insoluble $Cr(OH)_3$ at pH about 8. After this stage, the concentration of Cr(III) ions was decreased to 7.5 mg dm^{-3}.

The verification of theoretically calculated amounts of sorbent was carried out by using packed-bed column laboratory system with recirculation of the aqueous phase. By previous prediction of purification process, calculated dose of xCC needed for effective removal (RE 100%) of Cr(III) ions was 0.45 g dm^{-3} for 1.0 dm^{-3} of effluent with concentration 7.5 mg dm^{-3}. The effluent, with initial pH 5.0 and temperature 20 °C, was treated in packed-bed column with recirculation of the aqueous phase. After 10 min, concentration of Cr(III) ions decreased to 0.86 mg dm^{-3}; after 20 min, it was 0.21 mg dm^{-3}; and after 40 min, concentration of Cr(III) ions was lower than 0.1 mg dm^{-3}.

To test the efficiency of xCC for removal of MB from contaminated water, the river water was used as the matrix of the sorption solution. By previous prediction of purification process, calculated dose of xCC needed for complete removal (RE 100%) of MB was 1.20 g for 1.0 dm^{-3} of the river water contaminated with MB, with initial pH 5.0 and temperature

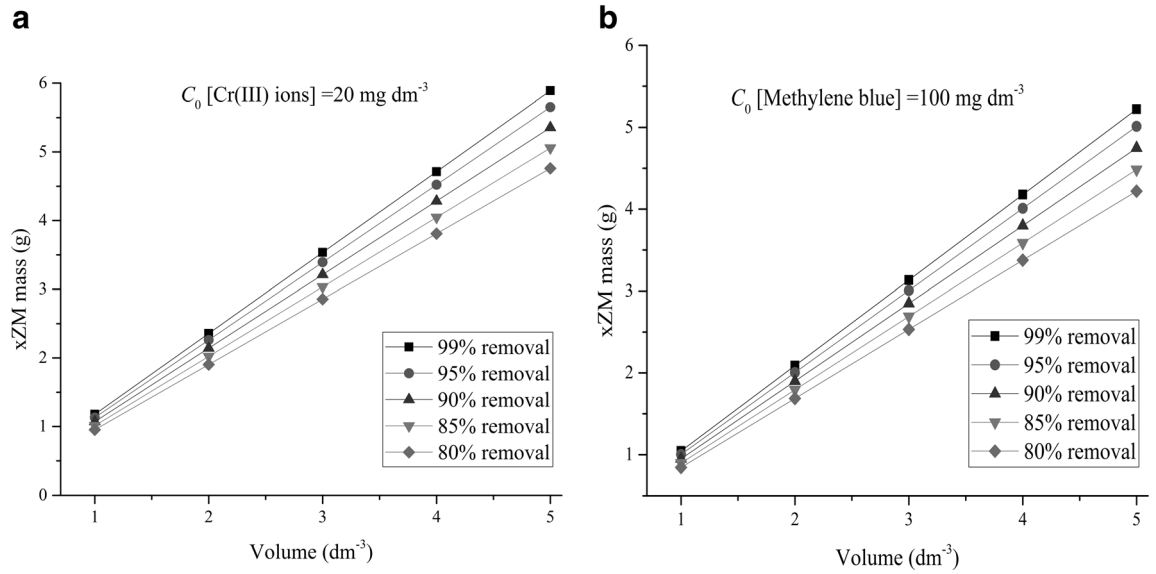

Fig. 8 The predicted amount of xCC for the sorption of **a** Cr(III) ions and **b** MB, at temperature 20 °C

20 °C. The concentration of MB in sample was 100 mg dm^{-3}. Treatment was conducted in system with packed-bed column with recirculation of the aqueous phase. Results have shown that removal of MB from contaminated river water was very effective. The removal efficiency was 90% after 20 min, and 94% after 40 min, which is in a relatively good agreement with predicted value. Slightly lower value of the removal efficiency occurs due to presence of other contaminants in river water (Ca(II), Mg(II), organic matter, etc.). Competition among ions for sorption sites could hinder xCC binding ability for MB, as expected. The high removal efficiency of MB in river water by xCC, indicates the great application potential of xanthated biosorbent in removing of cationic pollutants from water.

Conclusion

This study shows that the xanthated corn cob has high potential as an efficient biosorbent for the removal of Cr(III) and methylene blue from water. The presence of the sulfur functional group on the sorbent surface was confirmed by FTIR and EDX analysis. The Cr(III) intake by xCC was confirmed by EDX analysis. The kinetic experimental data fitted very well to pseudo-second order and Chrastil's kinetic models, i.e., the sorption is under both reaction and diffusion control. The Langmuir model can describe the equilibrium data for biosorption of Cr(III) ions onto xCC, and so the nature of sorption of Cr(III) ions on the sorbent is more compatible with Langmuir assumptions. However, the sorption of MB is better described with Brouers–Sotolongo isotherm model. The sorption mechanism of Cr(III) ions and MB onto xCC is a complex process, from one side because of different sizes and shapes of pores on sorption surface and from the other side because of different functional groups on the surface of xCC (xanthate, carboxylic, hydroxyl, and other groups). The sorption of Cr(III) and MB onto xCC occurs via different possible interactions, mainly electrostatic attraction, ion exchange, and complexation. Investigation of thermodynamics of the sorption of cations on xCC shows that process is endothermic, feasible, and spontaneous. The laboratory system with packed-bed column and recirculation of the aqueous phase, created in this study, can be used for purification of water in rinse baths in galvanization and similar processes, offering an alternative treatment for the removal of heavy metals and saving of process water.

The developed xCC biosorbent has demonstrated not only high sorption capacity and faster kinetics, but it also has additional benefits like simple synthesis, absence of secondary pollution, cost-effectiveness, and eco-friendliness. It can be proved to be a promising advanced sorbent for removal of cationic pollutants from contaminated natural and wastewaters. The regeneration and desorption aspect of xCC needs further studies for its real cost-effectiveness.

Acknowledgements The authors would like to thank the Ministry of Education, Science and Technological Development of the Republic of Serbia for supporting this work (Grant no. TR 34008).

References

Altenor S, Carene B, Emmanuel E, Lambert J, Ehrhardt JJ, Gaspard S (2009) Adsorption studies of methylene blue and phenol onto vetiver roots activated carbon prepared by chemical activation. J Hazard Mater 165:1029–1039

Anderson RA (1997) Chromium as an essential nutrient for humans. Regul Toxicol Pharmacol 26:S35–S41

Bennett GF (2001) Industrial waste treatment handbook: Frank Woodward, Butterworth-Heinemann, Woburn, MA doi:10.1016/S0304-3894(01)00391-0.

Carrillo F, Lis MJ, Colom X, López-Mesas M, Valldeperas J (2005) Effect of alkali pretreatment on cellulase hydrolysis of wheat straw: kinetic study. Process Biochem 40:3360–3364

Chojnacka K, Chojnacki A, Gorecka H (2005) Biosorption of Cr^{3+}, Cd^{2+} and Cu^{2+} ions by blue–green algae Spirulina sp.: kinetics, equilibrium and the mechanism of the process. Chemosphere 59:75–84

Chrastil J (1990) Adsorption of direct dyes on cotton: kinetics of dyeing from finite baths based on new information. Text Res J 60:413–416

Deniz F, Kepekci RA (2017) Bioremoval of malachite green from water sample by forestry waste mixture as potential biosorbent. Microchem J 132:172–178

El Nemr A, El-Sikaily A, Khaled A, Abdelwahab O (2015) Removal of toxic chromium from aqueous solution, wastewater and saline water by marine red alga *Pterocladia capillacea* and its activated carbon. Arab J Chem 8:105–117

Elabbas S, Mandi L, Berrekhis F, Pons MN, Leclerc JP, Ouazzani N (2016) Removal of Cr(III) from chrome tanning wastewater by adsorption using two natural carbonaceous materials: eggshell and powdered marble. J Environ Manag 166:589–595

Gilbert A, Emmanuel I, Adebanjo A, Olalere G (2011) Biosorptive removal of Pb^{2+} and Cd^{2+} onto novel biosorbent: defatted *Carica papaya* seeds. Biomass Bioenergy 35:2517–2525

Guiza S (2017) Biosorption of heavy metal from aqueous solution using cellulosic waste orange peel. Ecol Eng 99:134–140

Gupta VK, Agarwal SH, Saleh TA (2011) Chromium removal by combining the magnetic properties of iron oxide with adsorption properties of carbon nanotubes. Water Res 45:2207–2212

Hafshejani LD, Nasab SB, Gholami RM, Moradzadeh M, Izadpanah Z, Hafshejani SB, Bhatnagar A (2015) Removal of zinc and lead from aqueous solution by nanostructured cedar leaf ash as biosorbent. J Mol Liq 211:448–456

Haque MA, ShamsUd-Din M, Haque M (2002) The effect of aqueous extracted wheat bran on the baking quality of biscuit. Int J Food Sci Technol 37:453–462

Ho YS (2006) Isotherms for the sorption of lead onto peat: comparison of linear and non-linear methods. Pol J Environ Stud 15(1):81–86

Iftikhar AR, Bhatti HN, Hanif MA, Nadeem R (2009) Kinetic and thermodynamic aspects of Cu(II) and Cr(III) removal from aqueous solutions using rose waste biomass. J Hazard Mater 161:941–947

Karaoglu MH, Zor S, Ugurlu M (2010) Biosorption of Cr(III) from solutions using vineyard pruning waste. Chem Eng J 159:98–106

Kesraoui A, Moussa A, Ben Ali G, Seffen M (2016) Biosorption of alpacide blue from aqueous solution by lignocellulosic biomass: *Luffa cylindrica* fibers. Environ Sci Pollut Res 23:15832–15840

Khan AR, Ataullah R, Al-Haddad A (1997) Equilibrium adsorption studies of some aromatic pollutants from dilute aqueous solutions on activated carbon at different temperatures. J Colloid Interface Sci 194:154–165

Kostić M, Radović M, Mitrović J, Antonijević M, Bojić D, Petrović M, Bojić A (2013) Using xanthated *Lagenaria vulgaris* shell biosorbent for removal of Pb(II) ions from wastewater. J Iran Chem Soc 11(2): 565–578

Koutahzadeh N, Daneshvar E, Kousha M, Sohrabi MS, Bhatnagar A (2013) Biosorption of hexavalent chromium from aqueous solution by six brown macroalgae. Desalin Water Treat 51:6021–6030

Li C, Zhong H, Wang S, Xue J, Zhang Z (2015) Removal of basic dye (methylene blue) from aqueous solution using zeolite synthesized from electrolytic manganese residue. J Ind Eng Chem 23:344–352

Limousy L, Ghouma I, Ouederni A, Jeguirim M (2016) Amoxicillin removal from aqueous solution using activated carbon prepared by chemical activation of olive stone. Environ Sci Pollut Res. doi:10.1007/s11356-016-7404-8

Meseguer VF, Ortuño JF, Aguilar MI, Pinzón-Bedoya ML, Lloréns M, Sáez J, Pérez-Marín AB (2016) Biosorption of cadmium (II) from aqueous solutions by natural and modified non-living leaves of *Posidonia oceanica*. Environ Sci Pollut Res 23:24032–24046

Michalak I, Chojnacka K, Witek-Krowiak A (2013) State of the art for the biosorption process—a review. Appl Biochem Biotechnol 170: 1389–1416

Naja GM, Volesky B (2009) Treatment of metal-bearing effluents: removal and recovery. Heavy Met Environ:247–292

Özer A, Özer D, Özer A (2004) The adsorption of copper(II) ions on to dehydrated wheat bran (DWB): determination of the equilibrium and thermodynamic parameters. Process Biochem 39: 2183–2191

Park JH, Chon HT (2016) Characterization of cadmium biosorption by Exiguobacterium sp. isolated from farmland soil near Cu-Pb-Zn mine. Environ Sci Pollut Res 23:11814–11822

Puchana-Rosero MJ, Lima EC, Ortiz-Monsalve S, Mella B, da Costa D, Poll E, Gutterres M (2016) Fungal biomass as biosorbent for the removal of Acid Blue 161 dye in aqueous solution. Environ Sci Pollut Res. doi:10.1007/s11356-016-8153-4

Rafati L, Ehrampoush MH, Rafati AA, Mokhtari M, Mahvi AH (2016) Modeling of adsorption kinetic and equilibrium isotherms of naproxen onto functionalized nano-clay composite adsorbent. J Mol Liq 224:832–841

Rajput S, Pittman CU (2015) Magnetic magnetite (Fe_3O_4) nanoparticle synthesis and applications for lead (Pb^{2+}) and chromium (Cr^{6+}) removal from water. J Colloid Interface Sci 468:334–346

Rajurkar NS, Gokarn AN, Dimya K (2011) Adsorption of chromium(III), nickel(II), and copper(II) from aqueous solution by activated alumina. Clean Soil Air Water 39:767–773

Raval NP, Shah PU, Shah NK (2016) Adsorptive amputation of hazardous azo dye Congo red from wastewater: a critical review. Environ Sci Pollut Res 23:14810–14853

Sawalha MF, Peralta-Videa JR, Romero-González J, Gardea-Torresdey JL (2006) Biosorption of Cd(II), Cr(III), and Cr(VI) by saltbush (*Atriplex canescens*) biomass: thermodynamic and isotherm studies. J Colloid Interface Sci 300:100–104

Schiewer S, Volesky B (1995) Modelling of the proton–metal ion exchange in biosorption. Environ Sci Technol 29:3049–3058

Selatnia A, Bakhti MZ (2005) Biosorption of Cr^{3+} from aqueous solution by a NaOH-treated bacterial dead Streptomyces rimosus biomass. The European Journal of Mineral Processing and Environmental Protection 5:135–146

Selatnia A, Boukazoula A, Kechid N, Bakhti MZ, Chergui A, Kerchich Y (2004) Biosorption of lead(II) from aqueous solution by a bacterial dead Streptomyces rimosus biomass. Biochem Eng J 19:127–135

Singh CK, Sahu JN, Mahalik KK, Mohanty CR, Mohan BR, Meikap BC (2008) Studies on the removal of Pb(II) from wastewater by activated carbon developed from Tamarind wood activated with sulphuric acid. J Hazard Mater 153:221–228

Stanković M, Krstić N, Slipper I, Mitrović J, Radović M, Bojić D, Bojić A (2012) Chemically modified *Lagenaria vulgaris* as a biosorbent for the removal of Cu(II) from water. Austr J Chem 66(2):227–236

Wang J, Chen C (2009) Biosorbents for heavy metals removal and their future. Biotechnol Adv 27:195–226

Witek-Krowiak A, Harikishore Kumar Reddy D (2013) Removal of microelemental Cr(III) and Cu(II) by using soybean meal waste—unusual isotherms and insights of binding mechanism. Bioresour Technol 127:350–357

Woitovich Valetti N, Picó G (2016) Adsorption isotherms, kinetics and thermodynamic studies towards understanding the interaction between cross-linked alginate-guar gum matrix and chymotrypsin. J Chromatogr B 1012-1013:204–210

Yao L, Ye ZF, Tong MP, Lai P, Ni JR (2009) Removal of Cr^{3+} from aqueous solution by biosorption with aerobic granules. J Hazard Mater 165:250–255

Yun YS, Park D, Park JM, Volesky B (2001) Biosorption of trivalent chromium on the brown seaweed biomass. Environ Sci Technol 35:4353–4358